

A Complete Petrophysical-Evaluation Method for Tight Formations From Drill Cuttings Only in the Absence of Well Logs

Camilo Ortega, University of Calgary, Ecopetrol S.A.; and Roberto Aguilera, University of Calgary, China University of Petroleum, and Servipetrol Limited

Summary

The amount of tight-formation petrophysical work conducted at present in horizontal wells and the examples available in the literature are limited to only those wells that have complete data sets. This is very important. But the reality is that in the vast majority of horizontal wells, the data required for detailed analyses are quite scarce. Petrophysical evaluation in the absence of well logs and cores can now be considered owing to the possibility of measuring both the permeability and porosity of drill cuttings. This is essential because the application of the successive correlations used throughout the paper is based on porosity and permeability data.

To try to alleviate the data-scarcity problem, a new method is presented for complete petrophysical evaluation derived from information that can be extracted from drill cuttings in the absence of well logs. The cuttings data include porosity and permeability. The gamma ray and any other logs, if available, can help support the interpretation. However, the methodology is built strictly on data extracted from cuttings and can be used for horizontal, slanted, and vertical wells. The method is illustrated with the use of a tight gas formation in the Deep basin of the western Canada sedimentary basin (WCSB). However, it also has direct application in the case of liquids.

The method is shown to be a powerful petrophysical tool because it allows quantitative evaluation of water saturation, pore-throat aperture, capillary pressure, flow units, porosity (or cementation) exponent m , true-formation resistivity, and distance to a water table (if present). Also, the method allows one to distinguish the contributions from viscous and diffusion-like flow in tight gas formations. The method further allows the construction of Pickett plots without previous availability of well logs, and it assumes the existence of intervals at irreducible water saturation, which is the case of many tight formations currently under exploitation.

It is concluded that drill cuttings are a powerful direct source of information that allows complete and practical evaluation of tight reservoirs in which well logs are scarce. The uniqueness and practicality of this quantitative procedure originate from the fact that it starts only from the laboratory analysis of drill cuttings—something that has not been performed in the past.

Introduction

Petrophysics and log evaluation have advanced at a rapid pace in the oil and gas industry with the development of very sophisticated tools including imaging devices, core evaluation, and interpretation methods. Detailed analysis usually requires the use of several well logs. There are excellent methods for the evaluation of conventional and unconventional reservoirs including tight, shale, and coalbed-methane (CBM) reservoirs. There are also outstanding crossplots that contribute in many instances to a quick, yet accurate, formation evaluation by well logs. An example is provided by the Pickett plot (Pickett 1966, 1973) that has been

used for decades for the evaluation of sandstone and carbonate reservoirs and, more recently, for the analysis of shale-gas formations (Yu and Aguilera 2011).

There are instances, however, in which the amount of information is rather scarce. This is the case with some vertical wells and many horizontal wells. The data sets for some horizontal wells are quite complete in a few instances, permitting detailed petrophysical analysis. The reality, however, is that although the productivity of horizontal wells can be quite significant, in most cases the log data are quite scarce. This observation, stemming from conversations with various operators, inspired the development of a complete petrophysics method that is based solely on the measurements of porosity and permeability from drill cuttings. Using the cuttings, which are typically underused, constitutes a promising opportunity to complete evaluation or provide quick estimates. Obviously, logs and core data, when available, can and should be used for calibration purposes. However, the method developed in this paper uses as a foundation strictly information extracted from drill cuttings.

This implies that drill cuttings should be of good quality. We define a good-quality cutting as a sample with a size of 2 mm or more. However, on the basis of our experience in the laboratory, samples of 1 mm or more can provide good values of porosity and permeability (Solano 2010; Ortega 2012). Contreras (2011) has developed a drilling method that improves the quality of drill cuttings without sacrificing rate of penetration (ROP) in any significant way in the underpressured Deep basin of the WCSB, and he has shown the economic benefits of his approach.

Good-quality cuttings allow improved qualitative geologic analysis (Sneider and King 1984). They also can be used quantitatively for estimating key geomechanical properties such as Poisson's ratio and Young's modulus and for obtaining the estimation of a brittleness index (Ortega and Aguilera 2012a, b). These data are useful in a 3D hydraulic-fracturing simulation for designing multistage hydraulic-fracturing jobs in horizontal wells.

A methodology for a complete petrophysical evaluation of tight formations from drill cuttings only in the absence of well logs is developed in this paper.

Laboratory Work

The laboratory procedure starting with data collection has been summarized by Ortega and Aguilera (2012b) and is presented here for completeness. For a deeper treatment on the subject, refer to Ortega (2012) and Ortega and Aguilera (2012a). Chronologically, the steps are as follows:

- Sample collection
- Microscopic analysis
- Measureable-sample selection
- Cleaning and drying of samples
- Porosity measurement
- Permeability measurement

Sample Collection. Drill cuttings are available in many instances and provide a valuable direct source of information. They are collected generally every 5 m (16.4 ft) and sometimes every 2.5 m (8.2 ft). If drill cuttings are used, care should be taken by following the proposed methodology. In this case, the cuttings size

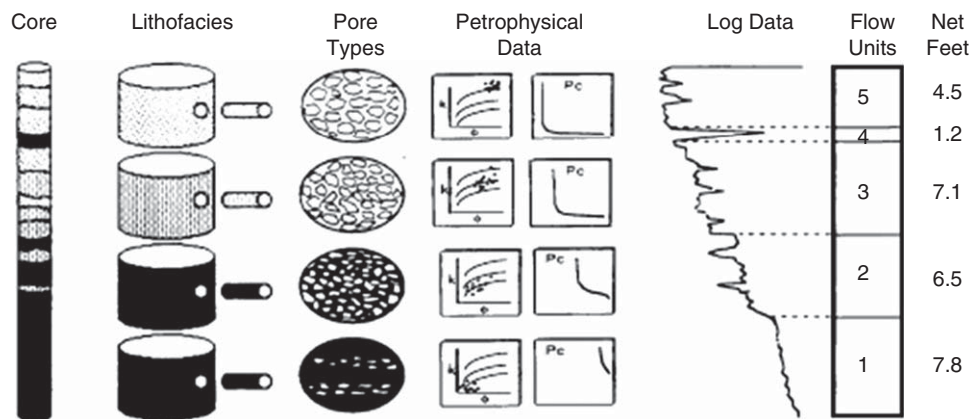


Fig. 1—Parameters commonly used for differentiating flow units (Hartmann and Beaumont 1999).

should be optimized (Contreras 2011) along with the sample volume and sample depth.

Microscopic Analysis. A key objective of the microscopic work, beyond the usual lithologic description, is the search for evidence of fracture porosity. Hews (2011) highlights some key features that provide good potential for pinpointing the existence of fracture porosity including fracture sets with mineral infill or lining; fracture sets with planar, unmineralized surfaces; and loose mineral crystals. We have been working on the location of the possible presence of fractures from cuttings for approximately 3 years with microscopic analysis. We find that cuttings are a good source of information for locating fractures in tight formations of the WCSB. But as with everything else related to cuttings, the information is not as robust as what can be obtained from cores and, in some cases, images. Furthermore, we do not know at this time if the proposed method would have application in the case of larger fractures and vuggy and karstic formations.

Measureable-Sample Selection. Ideally, cuttings chips larger than 2 mm are desired. However, chips larger than 1 mm generally provide reliable results (Solano 2010; Ortega 2012). After the cuttings are meshed, a selection is made by separating nonrock and nonreservoir fragments such as lost-circulation materials, metallic pieces, and shale fragments.

Cleaning and Drying. The procedure used is an adaptation from American Petroleum Institute Recommended Practice-40 (API RP-40 1998; Sections 3.6.4.4 and 4.3.1), which presents recommended practices for cores. Drilling-mud and reservoir-fluid information is required to select the optimal solvents for cleaning the cuttings (Culec 1977).

Porosity Measurement. The procedure follows the principles stated in API RP-40 (1998; Section 5.2.4) for core analysis. After the samples are dried, a saturation process is performed at vacuum conditions. A good comparison of laboratory porosity from cuttings and sonic log-derived porosity has been presented by Ortega and Aguilera (2012a, b).

Permeability Measurement. Permeabilities are determined with Darcylog equipment patented by the Institut Français du Pétrole and methodologies presented by Egermann et al. (2002, 2004, 2005) and Lenormand and Fonta (2007). Tight-gas-sandstone data (Ortega 2012) confirm the reliability of permeability measurements from cuttings. These permeabilities are most likely associated with the matrix system because many of the microfractures and slots in tight gas sandstones are probably not preserved in drill cuttings.

Interpretation. Porosity and permeability from drill cuttings have been used for calculating key geomechanical properties

(e.g., Poisson's ratio and Young's modulus) and for estimating a brittleness index. These data are useful for designing multistage hydraulic-fracturing jobs in horizontal wells (Ortega and Aguilera 2012a, b). The procedure for building a complete evaluation procedure on the basis of drill cuttings only is developed next in this paper and is explained with the use of data from the Deep basin of the WCSB tight gas sandstone.

Pore-Throat Aperture and Capillary Pressure

Hartmann and Beaumont (1999) set forth the meaning of a flow unit as "a reservoir subdivision defined on the basis of similar pore type." The determination of pore-throat aperture is one of the key parameters for characterizing reservoir rock. Fig. 1 shows some of the most important data currently used in the oil and gas industry for defining flow units.

Cores are mentioned explicitly (first column) as well as data and information that can be extracted from them (plugs, lithofacies, pore types, petrophysical data including capillary pressures). Also shown in Fig. 1 are log data, the interpreted flow units, and the net thickness of each flow unit. Note, however, that drill cuttings are not mentioned explicitly in Fig. 1. The new methodology developed in this paper allows the generation (on the basis of drill cuttings alone) of all the same data presented in Fig. 1 [i.e., lithofacies (from the study of cuttings and construction of thin sections), pore types, petrophysical data, log data (e.g., how to extract resistivity data is shown later in this paper; how to extract compressional and shear sonic data has been presented by Ortega and Aguilera 2012a, b), flow units, and net pay].

Knowledge of porosity, permeability, capillary pressure, and pore-throat aperture (and their relationship) is of considerable interest for reservoir engineers and petrophysicists because these parameters are directly related to fluid flow; and it is of interest for geologists who focus their interest primarily on the capability of rocks to behave as traps in the hydrocarbon-migration process (Pittman 1992).

As a result, a large amount of research has been carried out during the last few decades in an effort to establish the relationship and interdependence of these factors. Mercury-injection tests, although rather expensive and sometimes problematic because of environmental concerns, are shown to be a reliable method for estimating pore-throat-size distribution. Capillary pressure can be represented by (Washburn 1921)

$$P_c = -\frac{2\sigma\cos\theta}{r} \dots\dots\dots (1)$$

where P_c is capillary pressure (dynes/cm²), σ is surface tension (dynes/cm), θ is the contact angle, and r is the radius of pore aperture (μm).

H.D. Winland of the former Amoco's Research Department (Tulsa, Oklahoma) established in the 1980s empirical correlations that allow relating porosity and permeability with pore-throat size by use of (as a starting point) Eq. 1 and a data bank that included

TABLE 1—DEEP BASIN TIGHT-GAS-SANDSTONE POROSITY (ϕ) AND PERMEABILITY (k) FROM DRILL CUTTINGS (COLUMNS 3 AND 4) OBTAINED IN THE LABORATORY FOR WELL A^a

Sample	Bottom Depth MD (m)	Drill Cuttings			r_{p35} (μm)	S_{wi}	m	R_t	K_n	P_c (Hg-air) (psi)
		ϕ	K (md)							
1	3145.0	0.142	0.112	0.301	0.646	1.83	3	0.0004	363	
2	3150.0	0.083	0.196	0.495	0.096	1.87	330	0.0003	5,678	
3	3155.0	0.107	0.181	0.425	0.215	1.86	42	0.0003	1,666	
4	3160.0	0.178	0.194	0.349	0.965	1.81	1	0.0004	159	
5	3165.0	0.121	0.208	0.429	0.288	1.85	19	0.0003	1,004	
6	3170.0	0.088	0.310	0.591	0.092	1.87	313	0.0002	5,110	
7	3175.0	0.147	0.208	0.393	0.519	1.83	4	0.0003	403	
8	3180.0	0.154	0.182	0.362	0.643	1.83	3	0.0003	304	
9	3185.0	0.141	0.351	0.506	0.352	1.83	9	0.0002	607	
10	3190.0	0.093	0.164	0.433	0.149	1.87	111	0.0003	3,041	
11	3195.0	0.121	0.182	0.403	0.313	1.85	16	0.0003	929	
12	3197.5	0.083	0.038	0.237	0.216	1.87	72	0.0005	2,970	
13	3200.0	0.079	0.112	0.392	0.112	1.88	267	0.0003	5,476	
14	3205.0	0.102	0.116	0.356	0.232	1.86	40	0.0004	1,747	
Average		0.117	0.182			1.85				

^aThese data are used as a starting point to develop the new petrophysical-evaluation method introduced in this paper, which permits determination of r_{p35} , S_{wi} , m , R_t , K_n , and P_c (Hg-air) listed in Columns 5 through 10.

formations ranging in lithology and age from Ordovician to Tertiary, including Simpson, Delaware, Tensleep, Nugget, Cotton Valley, Muddy, Mesaverde, Terry, First Wall Creek, Frontier, Montrose, Vicksburg, and Frio sandstones (Pittman 1992). Winland's work was published by Kolodzie (1980) who used it to determine pay zones in Colorado (US) oil fields derived from pore-throat size. This led to refined values of original oil in place (OOIP) in his area of study. The empirical method developed by Winland to calculate the average pore-throat size on the basis of core porosity and permeability is represented by Eq. 2:

$$\log r_{35} = 0.732 + 0.588 \log k - 0.864 \log \phi \dots \dots \dots (2)$$

where r_{35} is the average pore-throat-aperture radius (microns) corresponding to a mercury saturation of 35% (or 35% cumulative pore volume) for a mixed combination of sandstone and carbonates, k is permeability in md, and ϕ is porosity (fraction). According to Pittman (1992), Winland ran regressions for different percentiles; the 35th one displayed the best correlation results. An excellent reference explaining the characterization of rock quality with r_{35} has been presented by Hartman and Beaumont (1999).

Kwon and Pickett (1975) developed an empirical correlation for mercury/air capillary pressure as a function of water saturation and the permeability/porosity ratio (k/ϕ) shown in Eq. 3 with 2,534 rock samples from 30 formations across North America, including sandstones and carbonates.

$$P_c = A \left(\frac{k}{100 \times \phi} \right)^{-B} \dots \dots \dots (3)$$

where P_c is mercury/air capillary pressure in psi, A is a function of water saturation as presented in Eq. 4 (A is the value of P_c in psi at $k/\phi = 1$ md/%), k is permeability in md, ϕ is porosity (fraction), and B is approximately equal to 0.45.

$$A = \text{constant } 1 \times S_w^{-\text{constant } 2} \dots \dots \dots (4)$$

where constant 1 has units of psi and constant 2 is dimensionless. Aguilera (2002) and Aguilera and Aguilera (2002) developed a similar equation for pore throat radius with the same data bank of 2,534 mercury/air capillary pressure measurements (Kwon and Pickett 1975). This radius, given by Eq. 5, was defined by Aguilera as r_{p35} to distinguish it from the Winland r_{35} . For practical purposes, results from r_{35} and r_{p35} provided approximately the

same results between 0.1 and 100 μm (Aguilera and Aguilera 2002). One advantage of Eq. 5 is that both porosity and permeability share the same exponent, making it possible to obtain simpler graphical correlations on log-log coordinates. For water-saturation values between 30 and 90%, Aguilera and Aguilera (2002) showed that the use of constant 1 = 19.5 and constant 2 = 1.7 in Eq. 4 provided good values of r_{p35} .

$$r_{p35} = 2.665 \left(\frac{k}{100 \times \phi} \right)^{0.45} \dots \dots \dots (5)$$

The methodology described previously was developed with data from cores. On the other hand, Eq. 5 has been used for calculating r_{p35} derived from porosities and permeabilities determined from drill cuttings in a vertical section of Well A and presented in the Drill Cuttings columns of **Table 1**. We are testing the correlations in vertical, slanted, and horizontal wells. We have found that the correlations are reliable for the tight formation that we are studying. However, for optimal results, these empirical correlations should be calibrated whenever possible with core data from the formation being evaluated. Results of the r_{p35} calculations are shown in the r_{p35} column of Table 1.

Flow (or Hydraulic) Units

Kolodzie (1980) based part of his work on Winland's research on the relationship between porosity, permeability, and pore-throat-aperture radius (r_{p35}) for improving his values of OOIP calculations. This was accomplished with pore-throat size as a cutoff for estimating whether a formation interval would be productive or not. As indicated previously, a flow unit is "a reservoir subdivision defined on the basis of similar pore type" (Hartmann and Beaumont 1999). Their classification with pore-throat apertures (r_{35}) proposed by Coalson et al. (1985) is presented in **Table 2**. The relationship between r_{35} and r_{p35} was established by Aguilera (2002) and is given in

$$r_{35} = 2.024 \times r_{p35} \left[\frac{k^{0.138}}{(100 \times \phi)^{0.414}} \right] \dots \dots \dots (6)$$

Aguilera and Aguilera (2002) consider the pore-throat aperture r_{p35} as a good approximation of mean hydraulic radius, which allows the providing of empirical estimates of initial oil rates (**Table 3**) for each flow unit as proposed by Martin et al. (1999).

TABLE 2—CLASSIFICATION BY PORE-THROAT (PORT) SIZE INITIALLY PROPOSED BY COALSON ET AL. (1985)

Port Category	Port-Size Range (r_{p35}) (μm)
Mega	>10
Macro	2–10
Meso	0.5–2
Micro	0.1–0.5
Nano	<0.1

TABLE 3—POSSIBLE LIQUID RATES DERIVED FROM PORT SIZE (AFTER MARTIN ET AL. 1999)

Port Category	Possible Liquid Rate (B/D)
Mega	>10,000
Macro	1,000–9,999
Meso	100–999
Micro	1–99
Nano	Mostly seal

These authors indicate that comparatively megaports can reach medium-gravity-oil-production rates of tens of thousands of barrels per day if “zonal thickness and other factors are constant;” without mechanical constraints, macroports can reach thousands of barrels per day; and mesoports can reach rates of hundreds of barrels per day. Microports can produce few to tens of barrels per day on pump. However, Martin et al. (1999) state that “microport flow units are decidedly nonreservoir in this comparative completion of moderate thickness and medium gravity oil without mechanical constraints. These flow units are of far more interest as potential seals for higher quality reservoir down dip.”

The concept has been extended to the case of gas rates by Deng et al. (2011). In the case of gas-well production rates, potentials reach more than a 100 MMscf/D for macro- and megaports, more than 10 MMscf/D for mesoports, more than 1 MMscf/D for microports, and more than 0.1 MMscf/D for nanoports (shale gas and CBM are not included in this preliminary estimate). The estimates are for vertical wells. In the case of low-permeability formations, the assumption is made that all wells are hydraulically fractured.

For the case of low-permeability gas reservoirs in horizontal wells, Deng et al. (2011) use the assumption that each fracturing stage is approximately equivalent, from the point of production rates, to a vertical well. In general, the same restrictions mentioned previously for oil, plus the big restriction of backpressures, apply to the preceding gas rates.

Fig. 2 shows a crossplot of permeability in a logarithmic scale vs. porosity in a Cartesian scale. There are lines for pore-throat

radii ranging between 20 and 0.00008 μm generated with Eq. 5. The lines of r_{p35} permit the development of flow units. The format of the graph was developed originally by H.D. Winland of Amoco (Kolodzie 1980) with data from carbonate and sandstone reservoirs.

Winland’s graph was modified by Aguilera and Aguilera (2002) with data from 2,534 sandstone and carbonate reservoirs in North America. The data bank included the Aux Vases, Hoover, Dakota, Nesson, Judith River, Lodgepole, Nisku dolomite, Morrow and Keyes, Hunton, Granite Wash, Venango, Cypress, Mission Canyon, Cherokee, Bartlesville, Stony Mountain, Swift, Muddy, Tar Springs, Minnelusa, Red River, Des Moines, Devonian, Benois, Trenton limestone, Silurian, and Edwards formations. The data bank had been used originally by Kwon and Pickett (1975) for creating a pore-structure model and developing pore-structure interrelationships.

Finally, data from tight-gas formations and shale-gas formations from various basins of North America permitted an extension to handle very low permeabilities (Aguilera 2010). Although not a panacea, the graph has since been extended to include data from tight and shale formations from the Middle East, North Africa, and the Perth basin in Australia.

The result of all this empirical work has led to the graph presented in Fig. 2. The graph has been developed to include conventional reservoirs, tight gas reservoirs, and shale-gas reservoirs (Aguilera 2010; Deng et al. 2011). Geological size classification of pore throats (ports at r_{p35}) includes megaports, macroports, mesoports, microports, nanoports, and picoports.

Knudsen number is used to distinguish between viscous and diffusion-like flow (Rahmanian et al. 2010; Ziarani and Aguilera 2012). The contribution of each viscous and diffusion-like flow can vary, depending on various properties including pore size, pressure, and temperature. Rahmanian et al. (2011) have presented a unified diffusion/viscous flow model with pore-level studies of tight gas formations.

The right-hand side of the graph includes the estimated oil and gas rates discussed previously. Although the emphasis of this paper is on gas reservoirs, the original use of the r_{p35} radii was in the estimation of oil rates (Martin et al. 1999). This integrated concept of port size and flow units might prove valuable, particularly in exploration areas and in those cases with a limited number of wells and limited information, in which values (or at least approximations) of porosity and permeability are available.

Irreducible Water Saturation

Morris and Biggs (1967) presented an empirical correlation (Eq. 7) to calculate the permeability of reservoirs at irreducible water saturation. This particular condition makes the application of their correlation reliable in the study area considered in this paper because wells producing from the tight gas sandstone under consideration (with no commingled production) in the Deep basin have produced water-free gas (Solano et al. 2011) during several years.

$$k^{1/2} = \frac{c \times \phi^3}{s_{wi}} \dots \dots \dots (7)$$

Morris and Biggs (1967) also corroborated Buckles’ (1965) observation that the product of porosity and water saturation was approximately constant for intervals at irreducible water

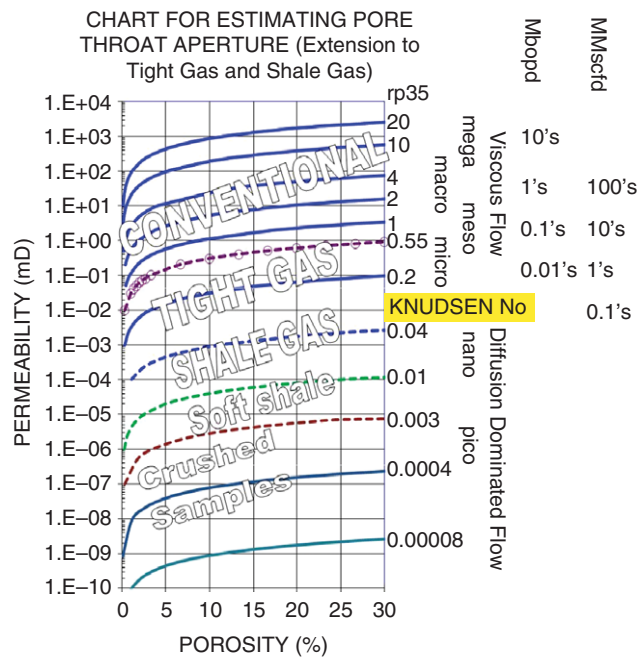


Fig. 2—Flow units as a function of pore-throat apertures (r_{p35}), porosities and permeabilities, and possible ranges of oil- (thousands of BOPD) and gas-flow rates (millions of scf/D) for different pore-throat apertures (Deng et al. 2011).

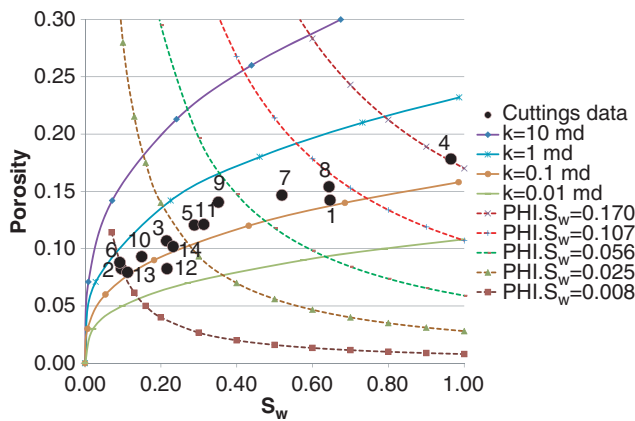


Fig. 3—Smooth solid lines representing constant permeability are a graphical expression of Eq. 8 for the case of dry gas. Dashed lines represent constant values of the product of porosity and water saturation [Buckles' number (Buckles 1965)]. Porosity and permeability from drill cuttings determined in the laboratory are represented by black dots. All data points are at irreducible water saturation.

saturation. Because porosity and permeability (Drill Cuttings columns in Table 1) are obtained from drill cuttings, and the tight gas formation being considered does not produce any water, it is possible to estimate irreducible water saturation with the use of

$$S_{wi} = \frac{c \times \phi^3}{k^{1/2}} \dots \dots \dots (8)$$

In Eqs. 7 and 8, k is permeability in millidarcies, ϕ is porosity (fraction), and c is a constant that depends on the density of the hydrocarbon filling the formation. For a medium-gravity oil (approximately 25°API), $c = 250$ and, for a dry gas, $c = 75$ to 79. Eq. 8 is presented as isopermeability curves in Fig. 3 for the dry-gas case. Black dots represent the irreducible-water-saturation values obtained with data from drill cuttings (S_{wi} column in Table 1). The graph also includes dashed lines that correspond to constant values of the product of porosity and water saturation. A conventional interpretation of the graph would suggest the presence of moveable water as Buckles' number (Buckles 1965) becomes larger. However, in this unconventional tight gas reservoir that does not produce any water, the shifting of the cuttings data toward larger values of Buckles' number is indicative of a very heterogeneous reservoir, something corroborated from detailed geologic studies (Solano et al. 2011). Calculated values of irreducible water saturation are listed in the S_{wi} column of Table 1.

Note that three values of irreducible water saturation exceed 0.6, among which one is equal to 0.965 (very close to 100% water saturation). Our review of 271 wells producing exclusively from this tight gas formation across an area of more than 15 000 km² for several years indicated a lack of production of any formation water at all (Solano et al. 2011). This indicates that the water is not moveable (i.e., it is at irreducible conditions even if some of the values of water saturation approach 100%).

Porosity (or Cementation) Exponent m

The exponent m is the so-called cementation exponent in the petrophysics literature. This is probably a misnomer deeply rooted in the literature because m depends on, in addition to cementation, many intrinsic rock characteristics such as tortuosity; matrix, fracture, and vuggy porosity; shape, sorting, and packing of individual grains; and also on environmental properties such as net stress on the rocks. Thus, our preference is to call m the porosity exponent. Byrnes et al. (2006) developed an empirical correlation for calculating m with laboratory experiments performed on core samples from the Mesaverde tight gas formation in the US.

The Byrnes et al. (2006) correlation is given by Eq. 9 and is used in this study. For application in other areas in which log and

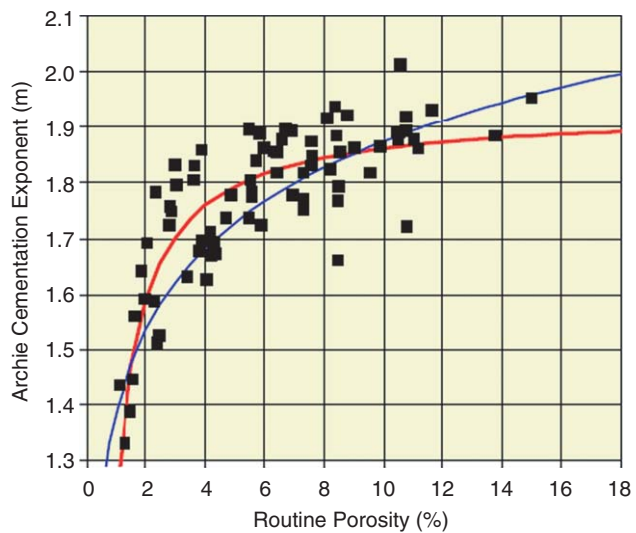


Fig. 4—Values of m from Mesaverde core data (black squares) and the Byrnes et al. (2006) empirical correlations (red and blue solid lines). The red line (Eq. 9) was used in this study.

core data are rather scarce, analogies and regional empirical correlations might be used.

$$m = 1.93 - \frac{0.68}{\phi} \dots \dots \dots (9)$$

A similar correlation (similar to Eq. 9) based on cores for the case of the tight gas sandstone being studied is not available at this time. However, this will be the subject of future laboratory work. Furthermore, there are some advances in this regard derived from petrographic and petrophysics work (Deng et al. 2011) that have indicated some similarities between the Mesaverde formation and the tight gas sandstones of the Deep basin, as shown in Fig. 4. Values of m for Well A calculated with the use of Eq. 9 are shown in Table 1.

The extension of drill-cuttings work to dual and triple porosity will be the subject of future work.

The amount of m values we have available for the tight gas formations in the WCSB is very limited. Because of this, we used m values from the Mesaverde tight gas formation that has an outstanding data bank (Byrnes et al. 2006) and presents some similarities with the formation considered in this study.

True-Formation Resistivity

Archie (1942) developed a relation among resistivity, saturation, and the formation factor, which is described by

$$S_w^{-n} = \frac{R_t}{F \times R_w} \dots \dots \dots (10)$$

Archie's equation applies to clean formations and provides a good approximation in the interval being considered in this study. However, in those cases in which shaliness is important, the value of R_t would have to be calculated from the selected shaly-formation equation. In that case, additional information would be needed such as shale volume and shale resistivity. Eq. 11 solves Archie's relation for calculating true-formation resistivity (R_t):

$$R_t = S_w^{-n} \times F \times R_w \dots \dots \dots (11)$$

In Eqs. 10 and 11, R_t and R_w are true-formation resistivity and water-formation resistivity (Ω -m), respectively, at reservoir temperature; m is the porosity (cementation) exponent; n is the water-saturation exponent (assumed equal to m); and F is the formation factor given by

$$F = a \times \phi^{-m} \dots \dots \dots (12)$$

TABLE 4—DATA USED FOR CALCULATING KNUDSEN NUMBER (K_n)

R_g (Gas)	8.314
N_A	6.03×10^{23}
P (Pa)	2.75×10^7
T (K)	373

With irreducible-water-saturation data and m values from Table 1, formation-water resistivity $R_w = 0.038 \Omega \cdot m$ (at $100^\circ C$ of temperature), and constant $a = 1$, values of R_t can be calculated with Eqs. 11 and 12. The unique aspect of this result is that R_t is calculated starting with data obtained in the laboratory with measurements on drill cuttings. Results are presented in the R_t column of Table 1.

The calculation of R_t is important because it allows possible comparison with other resistivity logs in the same general area and the construction of Pickett plots starting with drill cuttings only, as discussed later in this paper.

Distinguishing Between Viscous and Diffusion-Like Flow

The flow regime for a gas flowing through small pores can be established by calculating the Knudsen number (K_n). Knudsen number is defined in gas dynamics as the ratio of the molecular-mean-free path (λ) to a characteristic length (L), as shown in Eq. 13. λ is the average distance covered by a moving molecule between successive collisions that modify its direction or energy or other of its properties (Knudsen 1909, after Kennard 1938; Klinkenberg 1941; Rahmanian et al. 2013).

The characteristic length (L) depends on the flow geometry and the problem being considered. For this case, a tubular pore structure with a diameter d in meters is assumed, yielding Eq. 14. Pore-throat radius (in microns) r_{p35} is considered as representative of the microchannel radius leading to a Knudsen number calculated from Eq. 15.

$$K_n = \frac{\lambda}{L} \dots \dots \dots (13)$$

$$K_n = \frac{\lambda}{d} \dots \dots \dots (14)$$

$$K_n = \frac{10^6 \lambda}{2 \times r_{p35}} \dots \dots \dots (15)$$

λ is given by

$$\lambda = \frac{R_g \times T}{\sqrt{2} \times \pi \times N_A \times \delta^2 \times P} \dots \dots \dots (16)$$

where R_g is the universal gas constant ($Pa \cdot m^3/mol \cdot K$), T is temperature (K), N_A is Avogadro's number, δ is the collision diameter of the gas molecule (m), and P is pressure in the porous media (Pa).

Table 4 contains the basic data used for the calculations. Table 5 presents the gas mixture assumed to calculate the collision diameter. The gas mixture is assumed to be the same as used by Javadpour et al. (2007) because this is a good average for the

TABLE 5—GAS MIXTURE SELECTED FOR ESTIMATING COLLISION DIAMETER δ (m)

Gas Components	Mole (%)	Collision Diameter δ (m)	Molecular Weight (kg/kmol)
CH ₄	87.4	4.00×10^{-10}	16
C ₂ H ₆	0.12	5.20×10^{-10}	30
CO ₂	12.48	4.50×10^{-10}	44
Average		4.10×10^{-10}	19.5

area being studied. However, the collision diameter should be determined for each gas composition.

Four different flow regimes are recognized in literature for gas dynamics in porous media that can be identified with the Knudsen number. The limit for the validity of the continuum equations based on the Knudsen number is still a matter of study. There is an agreement on a gradual change of the flow behavior and the inexistence of a sharp transition. A common boundary between continuous and diffusion-like flow is considered to be on the order of $K_n = 0.01$.

Table 6 shows a classification of flow regimes derived from Knudsen-number values and includes a brief description of each flow regime. Calculated Knudsen numbers are presented in the K_n column of Table 1. For the tight gas sandstone presented in this study, continuum-flow conditions are dominant.

Note that with the quantitative methodology from drill cuttings developed in this paper, the Knudsen number is a function of pore-throat aperture (Eq. 15), which, in turn, depends on permeability and porosity (Eq. 5). Thus, the significant importance of k and ϕ from drill cuttings is displayed as an aid for determining the dominant type of flow, particularly in those cases in which cores and well logs are not available or are scarce. It is important to have an estimate of the Knudsen number because this provides an idea with respect to the type of flow in the reservoir (i.e., viscous or diffusion-like flow or maybe a combination of the two). A unified diffusion/viscous flow model with pore-level studies of tight gas formations has been developed by Rahmanian et al. (2013).

Estimation of Capillary Pressure

As discussed previously, capillary pressure is inversely related to pore-throat radius (Eq. 1). On the basis of work by Kwon and Pickett (1975) presented previously in Eq. 3, Aguilera (2002) developed an empirical correlation for mercury/air capillary pressure given in Eq. 17. Strictly, the results are valid for water saturations ranging between 30 and 90%. In practice, however, the range can be extended to larger and smaller water saturations.

$$P_c = (19.5 \times S_w^{-1.7}) \left[\frac{k}{(100 \times \phi)} \right]^{-0.45} \dots \dots \dots (17)$$

With permeability (md), porosity (fraction), and S_{wi} data in Table 1, it is possible to calculate drill-cuttings-based capillary pressures (psi) with the use of Eq. 17. Results are presented in the right-side column of Table 1. In this case, the S_{wi} values from Table 1 correspond also to S_w in Eq. 17 because several years of

TABLE 6—COMMON FLOW-REGIME CLASSIFICATION BASED ON KNUDSEN NUMBER (AFTER FLORENCE ET AL. 2007; ZIARANI AND AGUILERA 2012)

Regime	Knudsen-Number Range	Description
Continuum flow	$K_n < 0.01$	λ is negligible compared with L (d for this case). The continuum hypothesis of fluid mechanics is applicable.
Slip flow	$0.01 < K_n < 0.1$	λ is no longer negligible, and the slippage phenomenon appears.
Transition	$0.1 < K_n < 10$	Molecular approach starts to be required.
Free molecular flow	$K_n > 10$	Flow is dominated by diffusive effects.

For the case of geothermal reservoirs, the equation is

$$h \approx 0.205 \times P_c \quad \dots \dots \dots (20)$$

The constants for Eqs. 18 through 20 are average estimates for calculating approximate values of h with conventional reservoir-engineering methods. For example, for the case of a medium-gravity oil (Eq. 19) in which the difference between the specific gravity of water and oil is 0.27, mercury/air surface tension is 480 dynes/cm, oil/water surface tension is 35 dynes/cm, mercury/air contact angle is 140°, oil/water contact angle is 30°, and the water gradient is 0.433 psi/ft, the constant for calculating h is the inverse of $0.433 \times 0.27 \times [480 \times \cos(140)]/[35 \times \cos(30)] = 0.705$. The same approach is used for calculating the other average constant values.

Construction of Pickett Plots

Pickett plots (Pickett 1966, 1973) are powerful tools for petrophysical evaluation and log interpretation. They are widely used by geologists and reservoir engineers for reservoir characterization and estimations of hydrocarbons in place in sandstone, limestone, and dolomite reservoirs. Recent work by Yu and Aguilera (2011) shows important potential uses of Pickett plots for shale-gas reservoirs.

In this section, we introduce a method for building Pickett plots for tight gas formations in the absence of well logs. The method uses, as a starting point, the determination of porosity and permeability in the laboratory from drill cuttings with sizes larger than 1 mm. The procedure is derived from the observation that water in the Deep basin tight gas sandstone considered in this study exists at irreducible-saturation conditions. The assumption is made that a clean sandstone is used for experimental work in the laboratory. Furthermore, it is assumed that $n = m$, as mentioned previously in this paper. This assumption is useful in the tight gas formation considered in this study on the basis of our previous experience. However, if the value of n is known to be different from m , the Pickett plot can still be built with the procedure explained next. The porosity and permeability required for the construction of the Pickett Plot are shown in Table 1.

An average value of m equal to 1.85 (shown in Table 1) is used to determine the slope of the straight lines for constant water saturations in Pickett plots. The equation that yields the water-saturation straight lines in a log-log Pickett plot of porosity (y-axis) vs. true-formation resistivity (x-axis) is as follows (Pickett 1966, 1973):

$$\log(R_t) = -m \times \log(\phi) + \log(a R_w) \log(I) \quad \dots \dots \dots (21)$$

where I is the resistivity index given by

$$I = \frac{R_t}{F \times R_w} = S_w^{-n} \quad \dots \dots \dots (22)$$

The 100%-water-saturation straight line can be drawn by knowing the value of the slope of m , the formation water resistivity, and the value of a (used in Eq. 12). Archie (1942) assumed a to be equal to unity. However, later empirical studies have shown different values for a . Generally, log analysts try to determine values for m , n , and a for the particular rocks being evaluated. For the present work, a is assumed to be equal to unity, and as indicated previously, n is assumed equal to $m = 1.85$. The water resistivity R_w is equal to 0.038 Ω-m at reservoir temperature (100°C). Fig. 6 shows the drill-cuttings-based Pickett plot for the tight gas formation being considered built with the porosity and true-formation resistivity data shown in Table 1.

The cuttings data in Fig. 6 (black circles) follow a trend reminiscent of constant-permeability straight lines in Pickett plots given by the equation (Aguilera 1990)

$$\log(R_t) = (-3n - m) \times \log(\phi) + \log \left[a \times R_w \left(\frac{c}{k^2} \right)^{-n} \right] \quad \dots \dots \dots (23)$$

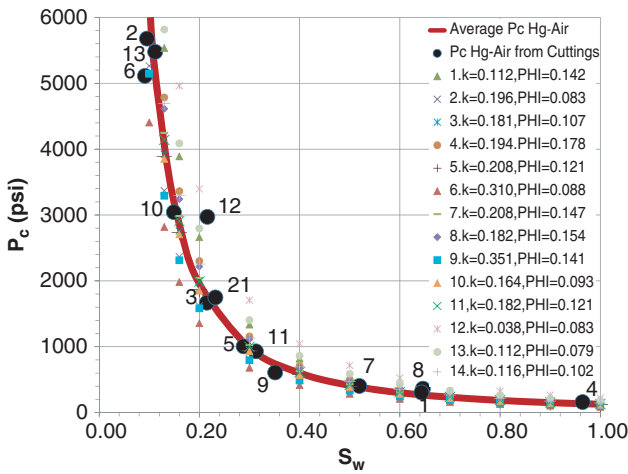


Fig. 5—Average drill-cuttings-based capillary pressure curve for Deep basin tight gas sandstone in Well A. Black dots represent data derived from drill cuttings collected at different depths. Symbols represent calculated capillary pressures from each cuttings sample.

actual production history have resulted in zero water production, indicating that water is nonmoveable in the formation being considered (Solano et al. 2011) even in zones with large values of water saturation.

An average capillary pressure curve developed from Eq. 17 with average porosity (0.117) and permeability (0.182 md) shown at the bottom of the Drill Cuttings columns in Table 1 is shown in Fig. 5. This average capillary pressure was used by Ramirez and Aguilera (2012) for the simulation of a tight gas formation in the Deep basin of Alberta (WCSB) (Masters 1979). Also shown in the graph are capillary pressures from individual drill-cuttings samples (black dots). Number 1 corresponds to the shallower cuttings sample; Number 14 corresponds to the deepest cuttings sample. Note that there is not order in the black dots with respect to depth. This highlights the heterogeneity of the formation also determined from Buckles' number (Fig. 3) and detailed geologic studies (Solano et al. 2011). Finally, the various symbols in Fig. 5 represent calculated individual capillary pressures derived from the laboratory permeability and porosity of each cuttings sample. Although theoretically there is a capillary pressure for each of the 14 samples, in practice for the case being studied, they are all close and allow the generation of one average capillary pressure. For values of permeability and porosity used in Eq. 17, refer to the legend box in Fig. 5.

For consistency with the 2,534 original capillary pressure mercury-injection tests used to develop the P_c empirical correlation used in this study (Aguilera 2002), Eq. 17 calculates mercury/air capillary pressure. However, in the case of tight gas formations, they are converted conventionally to air/gas capillary pressures (Ramirez and Aguilera 2012).

Location of Water Contact

Tight gas formations as discussed previously are continuous accumulations characterized by lack of a water leg (Law 2002). The method, however, can be extended to reservoirs in which water lies below the hydrocarbon-bearing zone, as shown by Aguilera (2002) and Aguilera and Aguilera (2002). For the case of dry gas, the approximate height of an interval at irreducible water saturation greater than the free-water level is given by

$$h \approx 0.405 \times P_c \quad \dots \dots \dots (18)$$

where h is height in feet above the free-water level at which capillary pressure is equal to zero and P_c is mercury/air capillary pressure in psi. For the case of medium-gravity (approximately 25° API) oil, the equation is

$$h \approx 0.705 \times P_c \quad \dots \dots \dots (19)$$

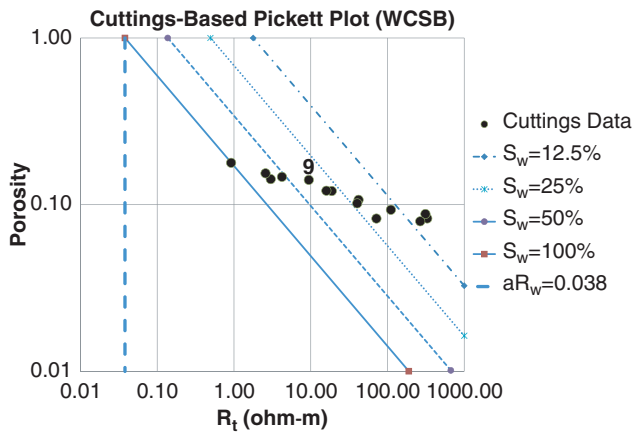


Fig. 6—Drill-cuttings-based Pickett plot for Deep basin tight gas sandstone in Well A.

where k is permeability in md. For a medium-gravity oil (approximately 25°API), $c = 250$, and for a dry gas, $c = 75$ to 79. The permeability from drill cuttings for Sample 9 (Table 1) is 0.351 md. Eq. 23 indicates that a crossplot of true resistivity (R_t) vs. porosity (ϕ) should result in a straight line with a slope equal $(-3n-m)$ for intervals with constant a , R_w , and k . If $n = m$, the slope is equal to $-4m$. Because the essence of the Pickett method is a log-log crossplot of ϕ vs. R_t , Eq. 23 indicates that lines of constant permeability can be built on the Pickett plot to make it a more complete formation-evaluation tool.

Fig. 7 is a repeat of Fig. 6 but now including lines of constant permeabilities equal to 0.003, 0.03, 0.3, and 3 md developed with the use of Eq. 23. Generally, the cuttings data fall between the constant-permeability lines equal to 0.03 and slightly more than 0.3 md, which corroborates the consistency of the drill cuttings-based Pickett plot and the measured permeabilities. The permeability of Sample 9 is 0.351 md.

Aguilera (2002) and Aguilera and Aguilera (2002) have presented the development of equations, methods, and examples on how to construct lines of constant capillary pressure and pore-throat radius on a Pickett plot. Strictly, the lines are valid between water saturations of 30 and 90%. However, our experience with the method shows that, in practice, the range can be extended to larger and smaller water saturations. The same methodology and the required equations have been used in this paper to construct the Pickett plots shown in Figs. 8 and 9. For example, Eq. 24 is used for building lines of constant capillary pressure (psi) in Fig. 8 (for the development of the equation, refer to Aguilera 2002):

$$\log(R_t) = (-m + 2.8125n)\log(\phi) + \log[aR_w(1.0961P_c^{-1.25})^{-n}] \dots \dots \dots (24)$$

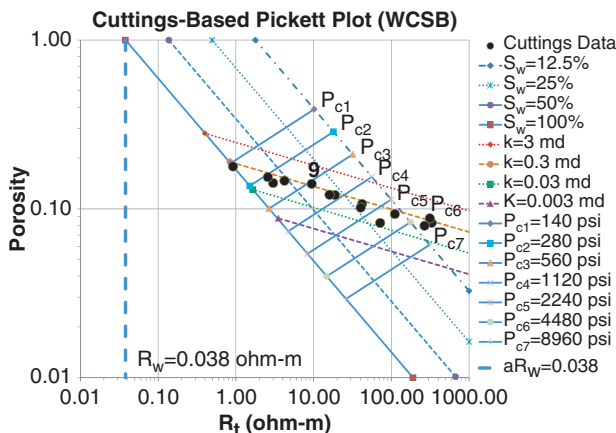


Fig. 8—Drill-cuttings-based Pickett plot including lines of constant capillary pressure for Deep basin tight gas sandstone in Well A.

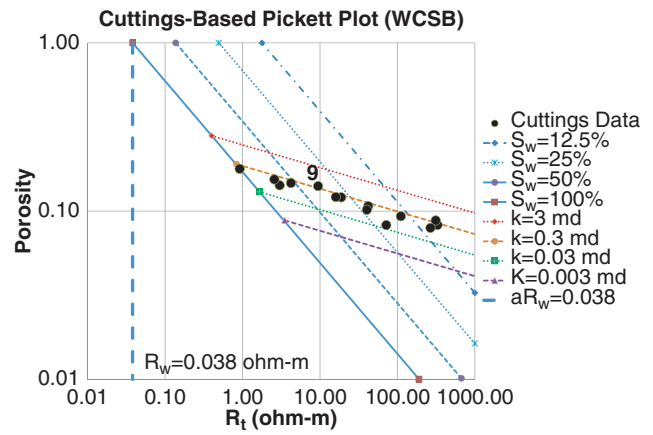


Fig. 7—Drill-cuttings-based Pickett plot including lines of constant permeability for Deep basin tight gas sandstone in Well A.

Eq. 24 indicates that a crossplot of R_t vs. ϕ on log-log coordinates should result in a straight line with a slope equal to $(-m + 2.8125n)$ for intervals at irreducible water saturation with constant aR_w and constant capillary pressure P_c , as shown in Fig. 8. Notice, for instance, that Sample 9 in Table 1 shows drill cuttings on the basis of a porosity of 0.141, a permeability of 0.351 md, a true-formation resistivity of 9 Ω -m, and a mercury/air capillary pressure of 607 psi. The location of Sample 9 in Fig. 8 corresponds to these values of porosity, permeability, true-formation resistivity, and capillary pressure.

Similarly, lines of constant pore-throat radius (microns) can be built on a Pickett plot as shown in Fig. 9 with the use of the following equation (for the development of the equation, refer to Aguilera 2002):

$$\log(R_t) = (-m + 2.8125n)\log(\phi) + \log\{aR_w[1.0961(108.1/r)^{-1.25}]^{-n}\} \dots \dots \dots (25)$$

Notice that Eqs. 24 and 25 are equivalent by making P_c equal to 108.1 divided by the pore-throat radius (r). This is correct when the mercury/air interfacial tension (IFT) is equal to 480 dyne/cm, and the mercury/air contact angle is equal to 140°. For different values of mercury/air IFT and contact angle, refer to the complete equation (Aguilera 2002). Eq. 25 indicates that a crossplot of R_t vs. ϕ on log-log coordinates should result in a straight line with a slope equal to $(-m + 2.8125n)$ for intervals at irreducible water saturation with constant aR_w and constant pore-throat radius r .

Pattern recognition is one of the main attributes that make Pickett plots so powerful. For example, Knudsen numbers can be built on a Pickett plot starting with Eq. 26 (Aguilera and Aguilera 2002):

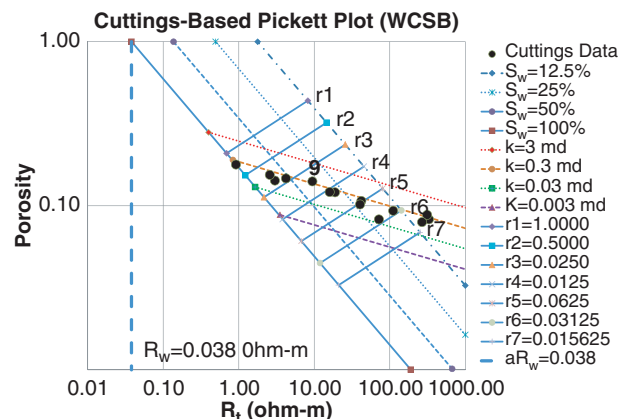


Fig. 9—Drill-cuttings-based Pickett plot including lines of constant pore radius for Deep basin tight gas sandstone in Well A.

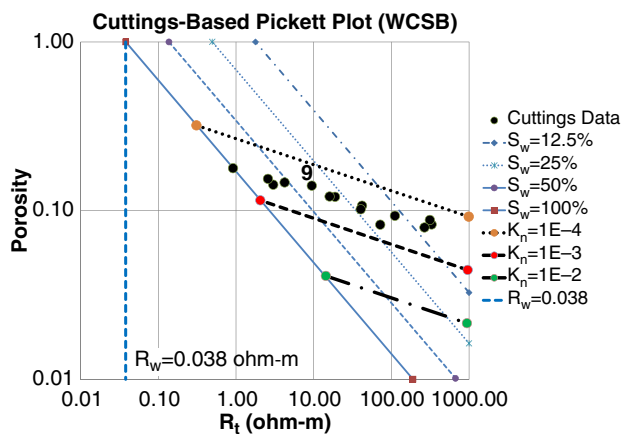


Fig. 10—Drill-cuttings-based Pickett plot including lines of constant Knudsen Number (K_n) for Deep basin tight gas sandstone in Well A. Knudsen numbers indicate that continuum (viscous) flow is the dominant flow regime in this reservoir.

$$\log(R_t) = (-2.5n - m)\log(\phi) + \log[aR_w(79)^{-n}(k/\phi)^{n/2}] \quad (26)$$

The ratio k/ϕ from Eq. 5 is given by

$$\frac{k}{\phi} = \left(\frac{r_{p35}}{2.665}\right)^{1/0.45} \times 100 \quad (27)$$

Inserting Eq. 27 into Eq. 26 leads to

$$\log(R_t) = (-2.5n - m)\log(\phi) + \log\left\{aR_w[79]^{-n}\left[100 \times \left(\frac{r_{p35}}{2.665}\right)^{1/0.45}\right]^{n/2}\right\} \quad (28)$$

The pore-throat radius (r_{p35}) from Eq. 15 is given by

$$r_{p35} = \frac{10^6 \lambda}{2K_n} \quad (29)$$

Inserting Eq. 29 into Eq. 28 leads to

$$\log(R_t) = (-2.5n - m)\log(\phi) + \log\left\{aR_w[79]^{-n}\left\{100 \times \left[\frac{10^6 \lambda}{2K_n}\right]^{1/0.45}\right\}^{n/2}\right\} \quad (30)$$

Eq. 30 is used for building lines of a constant Knudsen number on a Pickett plot, as shown on **Fig. 10**. Eq. 30 indicates that a crossplot of R_t vs. ϕ on log-log coordinates should result in a straight line with a slope equal to $(-2.5n - m)$ for intervals at irreducible water saturation with constant aR_w and constant Knudsen number K_n . Pattern recognition in **Fig. 10** shows that the drill-cuttings data fall between Knudsen numbers equal to 10^{-3} and 10^{-4} (i.e., for the tight-gas sandstone considered in this study, continuum-flow conditions are dominant). For instance, Sample 9 in **Table 1** shows a Knudsen number equal to 0.0002; the location of Sample 9 in **Fig. 10** corresponds to the same Knudsen number.

Discussion

The method developed for complete formation evaluation with the use of drill cuttings only in the absence of well logs is not meant to replace detailed petrophysical studies. But the method is useful as a strong complement, particularly in those cases in which log and core data are scarce. This happens sometimes in vertical wells but particularly in the case of many horizontal

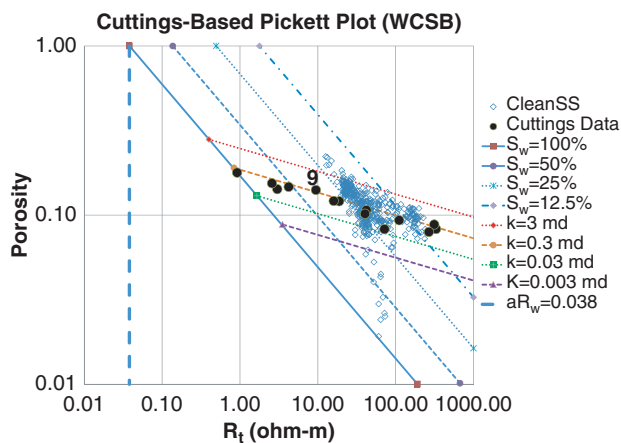


Fig. 11—Validation of Pickett plot from drill cuttings compared with logs from Well A.

wells. So far, the method has been tested in a single lithology (tight sandstone) in the WCSB. However, porosity and permeability have been determined from cuttings successfully for porosities larger than 5% in carbonates (Lenormand and Fonta 2007). This suggests the possibility that the proposed complete petrophysical-evaluation method might be extendable to carbonates. This is currently being investigated.

Obviously, for this method to work, the quality of the drill cuttings must be good. From experience we define a good-quality cutting as one with a diameter of at least 1 mm. Contreras (2011) and Contreras et al. (2012) have shown how to obtain good-quality drill cuttings without sacrificing drilling ROP in underpressured tight gas formations of the Deep basin (WCSB). With conditions of irreducible water saturation, the method developed in this paper allows quantitative evaluation of water saturation, pore-throat aperture, capillary pressure, flow units, porosity (or cementation) exponent m , true-formation resistivity, distance to a water table (if present), and the ability to distinguish the contributions from viscous and diffusion-like flow in tight gas formations.

The method also allows the construction of Pickett plots without previous availability of well logs. In addition to the conventional water saturation on Pickett plots, the method allows the construction of lines of constant permeability, constant capillary pressure, constant pore radius, and constant Knudsen number. If an aquifer is present, the method allows the estimation of the height to the water table.

Although not included in this paper, the method also can be used in the case of tight liquid reservoirs. The method permits further estimating of geomechanical properties such as Poisson's ratio and Young's modulus, as demonstrated by Ortega and Aguilera (2012a, b).

But the question remains: Although the petrophysical method from drill cuttings developed in this paper is mathematically correct and does not require the use of any well logs, how does it compare with log data if available? The answer is provided in **Fig. 11**, a repeat of **Fig. 7** but now including actual resistivity data and porosities calculated from a density log for the same interval evaluated with the drill cuttings. These log data are represented by the blue open diamonds. Because of the different spacing for collecting and reporting well-log and cuttings data, the comparison is considered very good, providing solid support to the method developed in this paper.

Although the cloud of resistivity/porosity points derived from a density log superposes some of the resistivity/porosity points derived from drill cuttings (black dots), one observes that a significant proportion of drill-cuttings points lies away from the density-log cloud (and the reciprocal assertion stands also for density-log points, but to a lesser extent if one considers the high number of density-log points). This is to be expected because of the significant scale difference between the well-log data (for example, a few centimeters) and the drill-cuttings sampling data

(250 to 500 cm). Because of these differences, the overall pattern of the Pickett plot is quite significant and supports the interpretation that uses drill cuttings.

Conclusions

Petrophysical evaluation in the absence of well logs and cores can now be considered owing to the possibility of measuring both the permeability and porosity of drill cuttings. This is essential because the application of the successive correlations used throughout the paper is derived from porosity and permeability data. The use of these data has led to the following conclusions:

- A new method has been developed for complete petrophysical evaluation with information that can be extracted from drill cuttings in the absence of well logs. The data from drill cuttings include porosity and permeability. The method has been illustrated with the use of a tight gas formation in the Deep basin of the WCSB.
- The method assumes the existence of intervals at irreducible water saturation, which is the case of many tight formations currently being exploited.
- The method is shown to be a powerful petrophysical tool because it allows a quantitative evaluation of water saturation, pore-throat aperture, capillary pressure, flow units, porosity (or cementation) exponent m , true-formation resistivity, and distance to a water table (if present), and it permits one to distinguish the contributions from viscous and diffusion-like flow in tight gas formations.
- The method allows the construction of Pickett plots and pattern recognition without previous availability of well logs. In addition to the standard water saturation, the method allows the introduction of lines of constant permeability, constant capillary pressure, constant pore-throat aperture, and constant Knudsen number on the Pickett plot.
- The uniqueness and practicality of this quantitative procedure are that it starts from laboratory analysis only of drill cuttings, something that has not been performed in the past. The results compare well with actual log measurements of porosity and resistivity.

Nomenclature

- a = constant in formation-factor equation, dimensionless
 A = empirical parameter, function of saturation (Kwon and Pickett 1975)
 c = constant, function of type of fluid (Morris and Biggs 1967)
 C = °C
 constant 1 = empirical constant (A determination)
 constant 2 = empirical constant (A determination)
 F = formation factor, dimensionless
 k = absolute permeability, md
 K_n = Knudsen number, dimensionless
 L = characteristic length (Knudsen-number calculation), m
 m = cementation (or porosity) exponent, dimensionless
 n = water-saturation exponent, dimensionless
 N_A = Avogadro's constant, 1/mol
 P = average reservoir pressure, Pa
 P_c = capillary pressure, psi
 PR = Poisson's ratio, fraction
 PR_{brit} = Poisson's ratio brittleness term, fraction
 r = radius of a capillary tube, μm
 r_{35} = Winland's average pore-throat radius at 35% mercury saturation, μm
 r_{p35} = average pore-throat radius at 35% mercury saturation, μ
 R_g = universal gas constant, Pa·m³/mol·K
 R_t = true-formation resistivity, $\Omega\cdot\text{m}$
 R_w = water resistivity, $\Omega\cdot\text{m}$
 S_w = water saturation, fraction
 S_{wi} = irreducible water saturation, fraction

- S_{wirr} = irreducible water saturation, fraction
 T = temperature, K
 δ = collision diameter, m
 θ = interface contact angle, degrees
 λ = molecular-mean-free path, m
 μ = viscosity, mPa·s
 ϕ = total porosity, fraction
 σ = interfacial tension, dyne/cm

Acknowledgments

Parts of this work were funded by the Natural Sciences and Engineering Research Council of Canada (NSERC agreement 347825-06), ConocoPhillips (agreement 4204638), Alberta Innovates Energy and Environment Solutions (AERI agreement 1711), the Schulich School of Engineering at the University of Calgary, and Servipetrol Limited. Darcylog equipment for measuring permeabilities from drill cuttings was provided by Roland Lenormand of Cydarex in Paris. Past and present GFREE team members at the University of Calgary provided valuable assistance throughout the development of this study. [Note: GFREE stands for an integrated multidisciplinary team researching geoscience (G), formation evaluation (F), reservoir drilling, completion and stimulation (R), reservoir engineering (RE), and economics and externalities (EE).] Their contributions are gratefully acknowledged.

References

- Aguilera, R. 1990. A New Approach for Analysis of the Nuclear Magnetic Log-Resistivity Combination. *J. Cdn. Pet. Tech.* **29** (1): 67–71. <http://dx.doi.org/10.2118/90-01-07-PA>.
- Aguilera, R. 2002. Incorporating Capillary Pressure, Pore Throat Aperture Radii, Height Above Free-Water Table, and Winland r_{35} Values on Pickett Plots. *AAPG Bull.* **86** (4): 605–624. <http://dx.doi.org/10.1306/61EEDB5C-173E-11D7-8645000102C1865D>.
- Aguilera, R. 2010. Flow Units: From Conventional to Tight Gas to Shale Gas Reservoirs. Paper SPE 132845 presented at the Trinidad and Tobago Energy Resources Conference, Port of Spain, Trinidad, 27–30 June. <http://dx.doi.org/10.2118/132845-MS>.
- Aguilera, R. and Aguilera, M.S. 2002. The Integration of Capillary Pressures and Pickett Plots for Determination of Flow Units and Reservoir Containers. *SPE Res Eval & Eng* **5** (6): 465–471. <http://dx.doi.org/10.2118/81196-PA>.
- American Petroleum Institute. 1998. *Recommended Practices for Core Analysis*, second edition, API-Recommended Practice 40, Washington, DC: American Petroleum Institute.
- Archie, G.E. 1942. The Electrical Resistivity Log as an Aid Determining Some Reservoir Characteristics. *Trans. AIME* **146** (1): 54–62. <http://dx.doi.org/10.2118/942054-G>.
- Buckles, R.S. 1965. Correlating and Averaging Connate Water Saturation Data. *J. Cdn. Pet. Tech.* **4** (1): 42–52. <http://dx.doi.org/10.2118/65-01-07-PA>.
- Byrnes, A.P., Cluff, R.M., and Webb, J.C. 2006. Analysis of Critical Permeability, Capillary Pressure, and Electrical Properties for Mesaverde Tight Gas Sandstone from Western US Basins. Quarterly Technical Progress Report, DOE Contract No. DE-FC26-05NT42660, Lawrence, Kansas: University of Kansas Center of Research.
- Coalson, E.B., Hartmann, D.J., and Thomas, J.B. 1985. Productive Characteristics of Common Reservoir Porosity Types. *South Texas Geological Society Bull.* **15** (6): 35–51.
- Contreras, O. 2011. An Innovative Approach for Pore Pressure Prediction and Drilling Optimization in the Abnormally Subpressured “Deep basin” of the western Canada Sedimentary Basin, MSc thesis, Department of Chemical and Petroleum Engineering, University of Calgary.
- Contreras, O., Hareland, G., and Aguilera, R. 2012. An Innovative Approach for Pore Pressure Prediction and Drilling Optimization in an Abnormally Subpressured Basin. *SPE Drill & Compl* **27** (4): 531–545. <http://dx.doi.org/10.2118/148947-PA>.
- Culec, L. 1977. Study of Problems Related to the Restoration of the Natural State of Core Samples. *J. Cdn. Pet. Tech.* **16** (4): 68–80. <http://dx.doi.org/10.2118/77-04-09-PA>.

- Deng, H., Leguizamon, J., and Aguilera, R. 2011. Petrophysics of Triple-Porosity Tight Gas Reservoirs With a Link to Gas Productivity. *SPE Res Eval & Eng* **14** (5): 566–577. <http://dx.doi.org/10.2118/144590-PA>.
- Egermann, P., Doerler, N., Fleury, M. et al. 2004. Petrophysical Measurements From Drill Cuttings an Added Value for the Reservoir Characterization Process. Paper SPE 88684 presented at Abu Dhabi International Petroleum Exhibition and Conference, Abu Dhabi, UAE, 10–13 October. <http://dx.doi.org/10.2118/88684-MS>.
- Egermann, P., Lenormand, R., Longeron, D. et al. 2002. A Fast and Direct Method of Permeability Measurements on Drill Cuttings. Paper SPE 77563 presented at the Annual Technical Conference and Exhibition, San Antonio, Texas, 29 September–2 October. <http://dx.doi.org/10.2118/77563-MS>.
- Egermann, P., Lenormand, R., Longeron, D. et al. 2005. A Fast and Direct Method of Permeability Measurement on Drill Cuttings. *SPE Res Eval & Eng* **8** (4): 269–275. <http://dx.doi.org/10.2118/77563-PA>.
- Florence, F.A., Rushing, J.A., Newsham, K.E., and Blasingame, T.A. 2007. Improved Permeability Prediction Relations for Low-Permeability Sands. SPE paper 107954 presented at the 2007 SPE Rocky Mountain Oil and Gas Technology Symposium, Denver, 16–18 April.
- Hartmann, D.J. and Beaumont, E.A. 1999. Predicting Reservoir System Quality and Performance. In *Exploring for Oil and Gas Traps: AAPG Treatise of Petroleum Geology, Handbook of Petroleum Geology*, ed. E.A. Beaumont and N.H. Foster, 9–1–9–154.
- Hews, P. 2011. Structural Features That Can Be Identified From Drill Cuttings. Geological Workshop Material, Calgary, Canada: Hara Consulting Ltd.
- Javadpour, F., Fisher, D., and Unsworth, M. 2007. Nanoscale Gas Flow in Shale Gas Sediments. *J. Cdn. Pet. Tech.* **46** (10). <http://dx.doi.org/10.2118/07-10-06-PA>.
- Kennard, E.H. 1938. *Kinetic Theory of Gases*. New York: McGraw Hill.
- Klinkenberg, L.J. 1941. The Permeability of Porous Media to Liquid and Gases. Paper 41-200 presented at the API 11th Mid-Year Meeting, Tulsa, Oklahoma, In *API Drilling and Production Practice*, Washington, DC: American Petroleum Institute, 200–213.
- Knudsen, M. 1909. *Ann. der Physik.* **28**: 75–130.
- Kolodzie, Jr., S. 1980. The Analysis of Pore Throat Size and Use of Waxman-Smits to Determine OOIP in Spindle Field, Colorado. SPE paper 9382 presented at the SPE Annual Technical Conference and Exhibition, Dallas, Texas, 21–24 September. <http://dx.doi.org/10.2118/9382-MS>.
- Kwon, B.S. and Pickett, G.R. 1975. *A New Pore Structure Model and Pore Structure Interrelationships: Society of Professional Well Log Analysts 16th Annual Logging Symposium*, 14 p.
- Law, B.E. 2002. Basin-Centered Gas Systems. *AAPG Bull.* **86**: 1891–1919.
- Lenormand, R. and Fonta, O. 2007. Advances in Measuring Porosity and Permeability From Drill Cuttings. Paper SPE 111286 presented at the 2007 SPE/EAGE Reservoir Characterization and Simulation Conference, Abu Dhabi, UAE, 28–31 October. <http://dx.doi.org/10.2118/111286-MS>.
- Martin, A.J., Solomon, S.T., and Hartmann, D.J. 1999. Characterization of Petrophysical Flow Units in Carbonate Reservoirs. *AAPG Bull.* **83**: 1164–1173.
- Masters, J.A. 1979. Deep Basin Gas Trap, Western Canada. *AAPG Bull.* **63**: 152–181.
- Morris, R.L. and Biggs, W.P. 1967. Using Log-Derived Values of Water Saturation and Porosity. Paper 1967-X presented at the Society of Professional Well Log Analysts Annual Logging Symposium, Denver, Colorado, 12–14 June.
- Ortega, C. 2012. Drill Cuttings-Based Methodology to Optimize Multi-Stage Hydraulic Fracturing in Horizontal Wells and Unconventional Gas Reservoirs, MSc thesis, Department of Chemical and Petroleum Engineering, Schulich School of Engineering, University of Calgary.
- Ortega, C. and Aguilera, R. 2012a. Use of Drill Cuttings for Improved Design of Hydraulic Fracturing Jobs in Horizontal Wells. Paper SPE 155746 prepared for presentation at the Americas Unconventional Resources Conference, Pittsburgh, Pennsylvania, 5–7 June. <http://dx.doi.org/10.2118/155746-MS>.
- Ortega, C. and Aguilera, R. 2012b. Potential Impact of Drill Cuttings on the Design of Multi-Stage Hydraulic Fracturing Jobs in Tight Gas Formations. Paper 2012-155 presented at the Society of Professional Well Log Analysts (SPWLA) 53rd Annual Logging Symposium, Cartagena, Colombia, 16–20 June. <http://dx.doi.org/10.2118/2012-155>.
- Pickett, G.R. 1966. A Review of Current Techniques for Determination of Water Saturation From Logs. *J. Pet. Tech* **18** (11): 1425–1433. <http://dx.doi.org/10.2118/1446-PA>.
- Pickett, G.R. 1973. Pattern Recognition as a Means of Formation Evaluation: Society of Professional Well Log Analysts 14th Annual Logging Symposium Transactions, paper A, p. A1A21.
- Pittman, E.D. 1992. Relationship of Porosity and Permeability to Various Parameters Derived from Mercury Injection—Capillary Pressure Curves for Sandstone. *AAPG Bull.* **76** (2): 191–198.
- Rahmanian, M.R., Aguilera, R., and Kantzas, A. 2013. A New Unified Diffusion-Viscous Flow Model Based on Pore Level Studies of Tight Gas Formations. *SPE J.* **18** (1): 38–49. <http://dx.doi.org/10.2118/149223-PA>.
- Rahmanian, M., Solano, N., and Aguilera, R. 2010. Storage and Output Flow From Shale and Tight Gas Reservoirs. Paper SPE 133611 presented at the SPE Western Regional Meeting, Anaheim, California, 27–29 May. <http://dx.doi.org/10.2118/133611-MS>.
- Ramirez, J.F. and Aguilera, R. 2012. Updip Water Blockage in the Nikanassin Basin Centered Gas Accumulation, Western Canada Sedimentary Basin. Paper SPE 162774 presented at the SPE Canadian Unconventional Resources Conference, Calgary, Alberta, Canada, 30 October–1 November. <http://dx.doi.org/10.2118/162774-MS>.
- Sneider, R.M. and King, H.R. 1984. Integrated Rock-Log Calibration in the Elmworth Field, Alberta, Canada: Part 1: Reservoir Rock Detection and Characterization. In *Elmworth: Case Study of a Deep Basin Gas Field: AAPG Memoir*, Vol. M 38, American Association of Petroleum Geologists Special Volumes, 205–214.
- Solano, N.A. 2010. Reservoir Characterization of the Upper Jurassic—Lower Cretaceous Nikanassin Group. MSc thesis, Geoscience Department, Geoscience Department, University of Calgary, Canada (December 2010).
- Solano, N., Zambrano, L., and Aguilera, R. 2011. Cumulative Gas Production Distribution on the Nikanassin Tight Gas Formation, Alberta and British Columbia, Canada. *SPE Res Eval & Eng* **14** (3): 357–376. <http://dx.doi.org/10.2118/132923-PA>.
- Washburn, E.W. 1921. Note on a Method of Determining the Distribution of Pore Sizes in a Porous Material. *Proceedings of the National Academy of Sciences of the United States of America (PNAS)* **7** (4): 115–116.
- Yu, G. and Aguilera, R. 2011. Use of Pickett Plots for Evaluation of Shale Gas Formations. Paper SPE 146948 presented at the SPE Annual Technical Conference and Exhibition, Denver, Colorado, 30 October–2 November. <http://dx.doi.org/10.2118/146948-MS>.
- Ziarani, A.S. and Aguilera, R. 2012. Knudsen's Permeability Correction for Tight Porous Media. *Transp. Porous Media (Springer)* **91** (1): 239–260. <http://dx.doi.org/10.1007/s11242-011-9842-6>.

Camilo E. Ortega holds a BS degree in petroleum engineering from the Universidad Nacional de Colombia and an MSc in petroleum engineering from the University of Calgary, Canada. He has worked as a field engineer in production testing and cased-hole logging in Colombia and worked as a work-over, completion, and stimulation engineer for Ecopetrol S.A. in Colombia. As a graduate student, Ortega was a member of the GFREE research team in the Schulich School of Engineering at the University of Calgary in which he focused on unconventional reservoir stimulation engineering in the Deep basin of the WCSB. He is currently working for Ecopetrol S.A. in Colombia as Senior Reservoir Engineer with emphasis on stimulation and unconventional resources. Ortega has written papers on unconventional reservoirs for SPE and the Society of Petrophysicists and Well-Log Analysts.

Roberto Aguilera is Professor and ConocoPhillips-NSERC-AIEE Chair in the Schulich School of Engineering, Chemical and Petroleum Engineering Department, the University of Calgary; Guest Professor at the China University of Petroleum (eastern China); and a principal of Servipetrol Limited in Canada. He heads the GFREE tight gas research program at the University

of Calgary. Aguilera is a petroleum engineering graduate from the Universidad de America at Bogota, Colombia, and holds MEng and PhD degrees in petroleum engineering from the Colorado School of Mines. He was an American Association of Petroleum Geologists instructor on the subject of naturally fractured reservoirs from 1984 through 1996. Aguilera has lectured, presented his course entitled Naturally Fractured Reservoirs, and/or has rendered consulting services in more than 50 countries throughout the world. He is a Distinguished

Author of the *SPE Journal of Canadian Petroleum Technology* (1993 and 1999), a recipient of the Outstanding Service Award (1994) and the Distinguished Service Medal (2006) from the Petroleum Society of CIM, an SPE Distinguished Lecturer on the subject of naturally fractured reservoirs for the 2000–2001 season, recipient of the 2011 SPE Canada Regional Distinguished Achievement Award for Petroleum Engineering Faculty, and past Executive Editor of the *SPE Journal of Canadian Petroleum Technology*.